# Supporting Information

## Amelio et al. 10.1073/pnas.1410609111

### SI Materials and Methods

**Mice.** All breeding and skin carcinogenesis were performed in the University Health Network (UHN) and approved by the UHN Animal Care Committe (ID:985 and 733). The two-step DMBA/PMA skin carcinogenesis model was used, using TAp73$^{+/+}$ and TAp73$^{-/-}$ mice of the C57B6/129Ola (F7) genetic background. The dorsal skin of 4-wk-old mice was exposed once to DMBA (25 μg in 0.1 mL), followed by biweekly exposure to PMA (6.25 μg in 0.1 mL of acetone) starting 2 wk after DMBA exposure. The tumor number and size were measured once per week. Analysis of genomic *TAp73* excision through PCR has been previously described (1). The experiment was performed on sex-matched, age-matched, and strain-matched mice (usually littermates).

**In Vivo Xenograft Tumor Model.** Mice were purchased from Charles River and then housed in the Central Research Facility of University of Leicester in accordance with UK legal guidelines. A total of $1.5 \times 10^6$ SaOs Tet on TAp73alfa was injected s.c. into 6–8-wk-old nude (nu/nu) mice in a one-to-one mix of RPMI:Matrigel (Gibco). Mice were treated by oral administration of 2 μg/mL doxycycline in water. A total of $2.5 \times 10^6$ shCTR or shTAp73 H1299 cells were injected s.c. into 6–8-wk-old nude (nu/nu) mice in a one-to-one mix of RPMI:Matrigel (Gibco). The tumors were measured using a caliper, and tumor volumes were calculated using the following formula: tumor volume ($mm^3$) = $4/3\pi \times \text{length}/2 \times \text{width}/2$. Microvessel density was determined by the number of microvessels per square millimeter. The experiment was performed on sex-matched, age-matched, and strain-matched mice.

**Aortic Ring Assay.** Thoracic aortas were removed from 8–12-wk-old TAp73$^{+/+}$ and TAP73$^{-/-}$ mice, and the fibroadipose tissue was dissected away. Forty-eight-well culture dishes were coated with 100 μL BME and allowed to solidify. The aortas were sectioned in 1-mm-long aortic rings, sealed in place with an overlay of 70 μL of BME, and covered with 300 μL endothelial basal medium (Clonetics) with 5% FCS or M199 with 10% FCS with VEGF-A (final concentration, 20 ng/mL; R&D Systems) and FGF-2 (final concentration, 10 ng/mL; R&D Systems). Tubular structures were examined using a phase contrast microscope (Axiovert 200M, Zeiss) and photographed. The lengths and projected areas of the capillary-like structures were then quantified.

**Immunofluorescence and Histological Analyses.** Mouse tumor tissues were embedded in frozen specimen medium (Criomatix; Shandon) or fixed in 4% paraformaldehyde (48 h) and embedded in paraffin. Nonspecific antigens were blocked by incubation in 5% goat serum in PBS for 1 h in a humidified atmosphere at room temperature. Subsequently, the sections were incubated for 1 h with anti-K14 (PRB-115P, Covance) and rhodamine Griffonia simplicifolia lectin (RL-1102, Vector Laboratories), washed three times with PBS, and incubated, if required, for 1 h with Alexa Fluor 488 secondary antibodies (Molecular Probes; Invitrogen). The tissue sections were counterstained with DAPI to highlight the nuclei. Fluorescence was evaluated through confocal microscopy (LSM 510, Zeiss), fitted with an argon laser (488 nm excitation), He/Ne laser (542 nm excitation), and UV excitation at 405 nm. Hematoxylin-eosin staining was performed as previously described (2) on paraffin-embedded sections to allow for the morphologic analysis of tumor samples. In brief, after deparaffinization and rehydration, the sections were stained for 5 min with hematoxylin and then washed in distilled water for 3 min and incubated 1 min in 1% HCl/70% alcohol. The sections were then washed in distilled water and stained 1 min in 1% eosin. The images were captured with a microscope (Axioplan 2, Zeiss) equipped with a camera. Microscopy images shown are representative of the biological group.

**Patient Samples.** Primary human tumor specimens with the histologic diagnosis of lung carcinomas were collected during surgery. The use of tissues and clinical data for this study was approved by the ethical committee of the University of Rome Tor Vergata (Rome, Italy). The committee stated that informed consent was not required because this study involved only a retrospective analysis of discarded tissue collected in the course of routine clinical care. Total protein preparation was performed on macrodissected tumor-enriched portions after pathology review. TAp73, HIF-1α, and VEGF-A quantification from tumor samples was performed through Western blot analyses.

**Cell Culture and Reagents.** The cells were cultured at 37 °C in 5% $CO_2$ in culture medium. H1299 and SaOs-2 cell lines were purchased from ATCC. H1299 and SaOs Tet-On cells were maintained in RPMI medium 1640 (Gibco) supplemented with 10% FCS, 250 mM L-glutamine, 50 mM 2-mercaptoethanol, penicillin/streptomycin (1 U/mL), nonessential amino acids, and 1 mM pyruvate (Invitrogen). RCC4 and RCC4/VHL cells were cultivated in DMEM 10% FBS. The temperature-sensitive ts20 Balb/C 3T3 clone A31 and H38 cell lines were a gift from H. Ozer, NJMS-UH Cancer Center, New Jersey Medical School, Newark, NJ, and C. Borner, Institute of Molecular Medicine and Cell Research Center for Biochemistry and Molecular Cell Research (ZBMZ), Freiburg, Germany, and were maintained in DMEM with 10% FBS at the permissive temperature of 34 °C. *Mycoplasma* test was performed routinely to verify the studies were not performed in the presence of mycoplasma contamination. For the ubiquitin-dependent degradation of HIF-1α, ts20 and H38 cells were transfected with the indicated plasmids and placed at 39 °C (to inactivate E1 enzyme) for 24 h. A parallel experiment was run at 34 °C as a control. The experiments with proteasomal inhibition were performed with 4 h MG132 treatment (20 μM; Sigma). The HIF-1α half-life analysis was performed in H1299 cells after HIF-1α stabilization with 4 h CoCl treatment (800 μM; Sigma) by performing a time course experiment using cycloheximide (100 μM; Sigma).

**Cell Transfection and Plasmid Vectors.** H1299 were transfected using Lipofectamine 2000 (Invitrogen), with the following overexpression constructs for HIF-1α wt: HIF-1α PA, TAp73α, TAp73β, or ΔNp73α. Expression vectors with different domains of HIF-1α wt were obtained by molecular cloning from pCMV6-Myc-HIF-1α, amplifying the fragments with the following primers: HIF-1α$^{1–330}$ forward primer, CCCCGCGATCGCCATGGAGGGCGCCGGCGGC, reverse primer CCCCACGCGTAGAATTCTTGGTGTTATATATGACA; HIF-1α$^{401–608}$ forward primer, CCCCGCGATCGCCATGGCCCCAGCCGCTGGAGAC, reverse primer CCCCACGCGTTTGTATTTGAGTCTGCTGGAATAC; HIF-1α$^{401–530}$ forward primer, CCCCGCGATCGCCATGGCCCCAGCCGCTGGAGAC, reverse primer CCCCACGCGTTTCATTGACCATATCACTATCCA; HIF-1α$^{610–826}$ forward primer, CCCCGCGATCGCCATGCCTACTGCTAATGCCACCAC, reverse primer CCCCACGCGTGTTAACTTGATCCAAAGCTCTG. Insertion in the pCMV6-Entry plasmid has been performed by T4 DNA ligase reaction (New England Biolabs) after enzymatic

reaction of fragments and vector with SgfI and MluI restriction enzymes (New England Biolabs). siRNA transfection was performed using Lipofectamine RNAiMAX (Invitrogen) with Silencer Predesigned TP73 (Invitrogen, product code AM16706), Silencer Validated RNA MDM2 (Invitrogen, product code AM51331), or Silencer Negative Control (Invitrogen). RCC4, RCC4/VHL, Ts20, and H38 cell lines were transfected with the indicated plasmids, using JetPrime transfection reagent (PolyPlus).

**Hypoxia Incubation.** The tumor cell lines were cultured in regular plates and placed in a modular incubator chamber (In vivo 200, Ruskinn) with continuous infusion of a preanalyzed gas mixture (94% N2, 5% $CO_2$, 1% $O_2$) at 37 °C. Chemical induction of HIF-1α was induced after treatment with $CoCl_2$ (Sigma-Aldrich).

**Immunoprecipitation and Western Blot.** Immunoprecipitation of endogenous proteins has been performed after 6 h of cisplatin (20 μM; Sigma), CoCl (800 μM; Sigma), and MG132 (20 μM; Sigma) by incubating ON at 4 °C with anti-p73 (Imgenex) and then 1 h at 4 °C with Protein G-Agarose (Roche). The beads were washed three times with Triton buffer, resuspended in Laemmli sample buffer, and incubated at 98 °C for 5 min before loading on SDS/PAGE protein gels. For immunoprecipitation of overexpressed proteins, the lysates (0.5 mg) were incubated ON at 4 °C with Ez view Red anti-HA affinity gel (E6779, Sigma) or Myc-Tag Sepharose beads (3400S, Cell Signaling). The beads were washed three times with Triton buffer, resuspended in Laemmli sample buffer, and incubated at 98 °C for 5 min before loading on SDS/PAGE protein gels. Immunoblotting was performed using standard protocols with the following primary Abs: mouse anti-GAPDH (G8795, Sigma), mouse anti-actin (A2228, Sigma), mouse anti-MDM2 (MG308, Sigma), mouse anti-HIF-1α (NB100-105, BD), mouse anti-HA (MMS-101P-503, Covance), mouse anti-VEGF-A (SAB3300042-100UL, Sigma), and rabbit anti-p73 [Melino Lab, as previously described (3)].

**Microarray Analysis.** RNA was extracted from tumor xenograft samples, using TRIzol (Invitrogen). RNA was reverse transcribed, converted to cRNA, amplified, and labeled with a cyanine-3 dye using a Low Input Quick Amp labeling kit from Agilent. Labeled cRNAs were hybridized to human gene expression microarrays (Agilent, catalog number G4851B), which contain 50,599 unique probes. The slides were washed using the Agilent wash buffer reagents and scanned with a G2505C Agilent Microarray Scanner (scan control version A.8.4.1). The data were extracted using the Agilent Feature Extraction software (version 10.7.3.1) and analyzed using Agilent GeneSpring GX software (version 12.1). To analyze significant differential expression, an unpaired Student's *t* test with Benjamini-Hochberg multiple testing correction was applied. mRNAs with a *P* value of less than or equal to 0.05 and a fold change of greater than 1.5 were considered to be both statistically and biologically significant.

**RNA Extraction, Reverse Transcription, and qPCR Analysis.** The RNA from cell pellets was extracted with an RNAeasy Kit (Qiagen); the RNA from mouse specimens was extracted using TRIzol (Invitrogen). The cDNA was reversed transcribed, using a RevertAid H Minus First Strand cDNA synthesis kit (Thermo Scientific), and the relative quantification was obtained through real-time qPCR, using the Power SYBR Green PCR Mastermix (Applied Biosystems).

**Statistics.** Data are presented as the mean values, and the error bars indicate ± SD. The number of biological replicates per experimental variable ($n$) is indicated in the figure legends. Statistical analyses were determined by the unpaired two-tailed Student's *t* test. The 0.05 level of confidence ($P < 0.05$) was accepted for statistical significance, and *P* values of each experiment are indicated in the figure legends. The investigators gathering quantitative data on mouse samples were blinded to the sample identities at the time of analysis. These images are representative of at least three independent experiments of the animal group.

**Bioinformatic Analyses.** A publicly available dataset (GSE31120) was used for the analysis of gene expression microarrays in primary human lung adenocarcinomas. The samples were then clustered by the expression of the TAp73 and ΔNp73probes. We used an unsupervised Bayesian clustering methodology. This method finds an optimal number of clusters and optimal clustering from an input of various preclusterings generated by a library of standard clustering methods. Optimization is based on a Bayesian formulation of a Gaussian mixture model. Signature scores were calculated using gene set enrichment analyses. Kaplan-Meier analysis was performed using the Matlab routine kmplot.

For the analysis of HIF-1/VEGF-A correlation in the p73 high-expression and p73 low-expression groups, the samples were split on the basis of the p73 normalized expression values. The absolute value of the Pearson correlation coefficient between the expression profile of HIF-1a and the expression profiles of its target VEGF-A were computed in both groups. To demonstrate that the differences in the correlations in both groups were significant, we used a Monte Carlo simulation, which is commonly used in biological studies when the null distribution cannot be derived analytically. The samples from the metadataset were split randomly into groups in the same proportion as in original split, based on p73 expression value. The correlation between HIF-1 and its target was computed, and the difference (absolute value) was computed for each pair (HIF-1 > VEGF-A). The procedure was repeated 1,000 times, generating a background distribution of difference in correlation between randomly sampled groups. The difference in correlation between HIF-1 and its targets for original split of samples, based on p73 expression value, was compared with the generated distribution. In most cases, in no one case of random split was the difference in correlation coefficients greater or equal to the one related to the original split, according to the p73 expression value.


1. Vikhanskaya F, et al. (2001) p73 Overexpression increases VEGF and reduces thrombospondin-1 production: Implications for tumor angiogenesis. *Oncogene* 20(50): 7293–7300.
2. Amelio I, et al. (2012) miR-24 triggers epidermal differentiation by controlling actin adhesion and cell migration. *J Cell Biol* 199(2):347–363.
3. Sayan AE, et al. (2005) New antibodies recognizing p73: comparison with commercial antibodies. *Biochem Biophys Res Commun* 330(1):186–193.

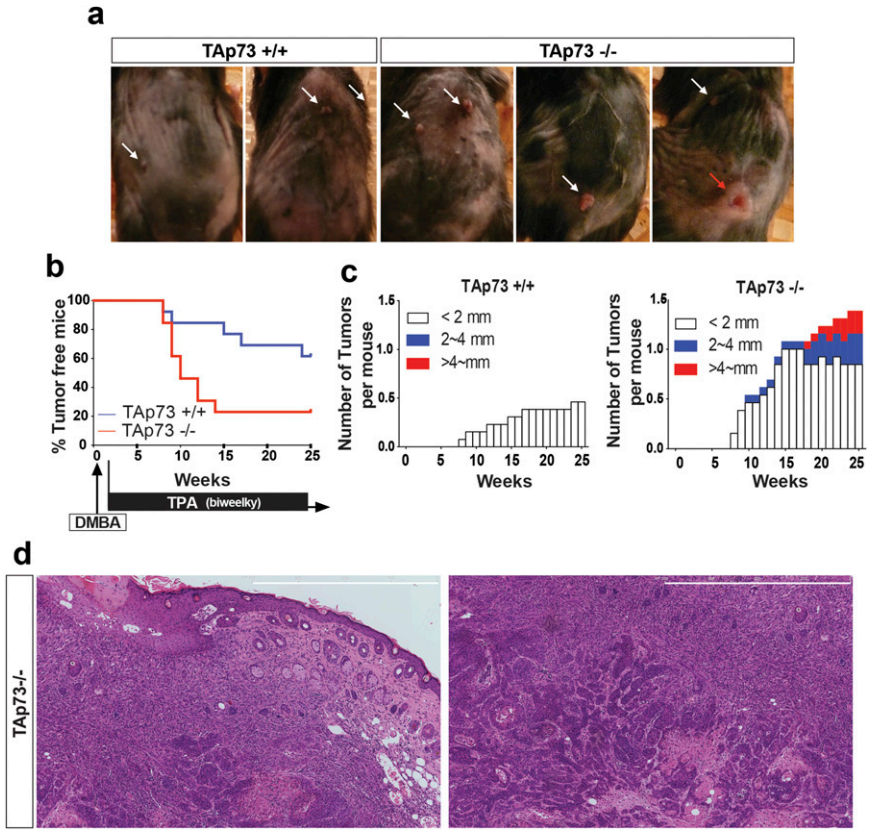


**Fig. S1.** (*A* and *B*) TAp73$^{-/-}$ mice show an increased number of tumors ($n = 13$ per genotype, Log rank *t* test, $P = 0.022$). An initial dose of the chemical initiator mutagen 7,12-dimethylbenz[a]anthracene was followed by repeated applications of a proinflammatory phorbol ester, 12-O-tetradecanoyl-phorbol 13-acetate. (*C*) Tumors from TAp73$^{-/-}$ mice are significantly larger compared with those of their TAp73$^{+/+}$ littermates. ($n = 13$ per genotype). (*D*) Hematoxylin/eosin staining of poorly differentiated skin squamous cell carcinoma from TAp73$^{-/-}$ mice. (Scale bars, 800 μm.)

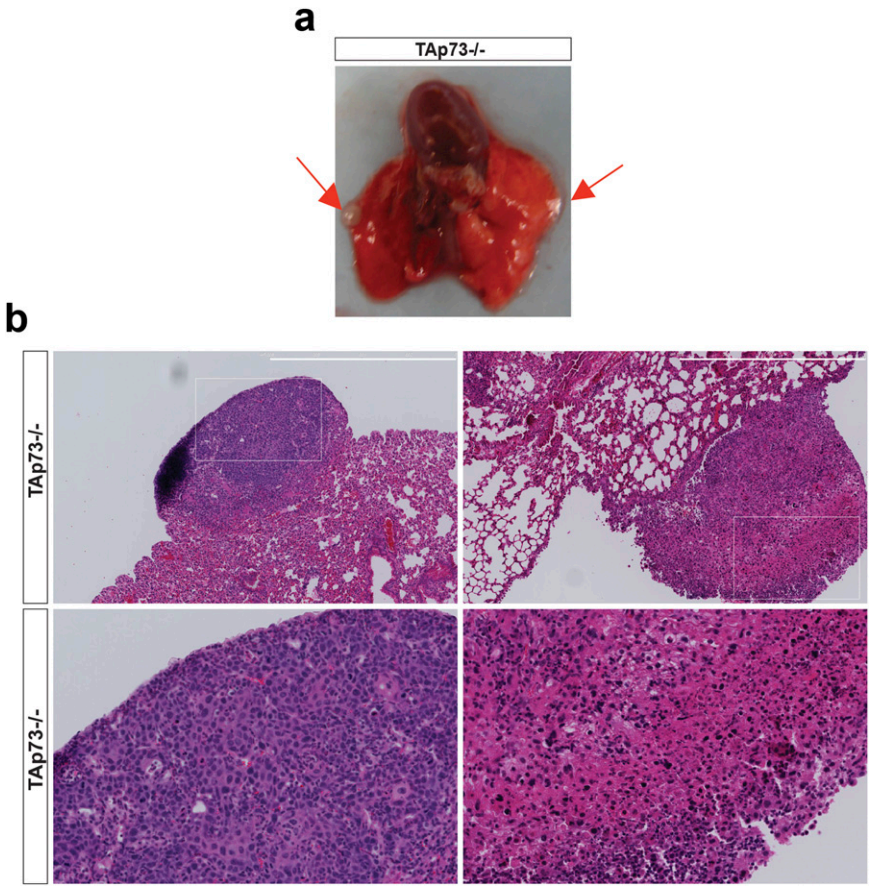


**Fig. S2.** (*A*) Lungs from TAp73$^{-/-}$ mice show malignant lesions. (*B*) Hematoxylin/eosin staining of TAp73$^{-/-}$ mouse lung revealed lung lesions. (Scale bars, 800 μm.)

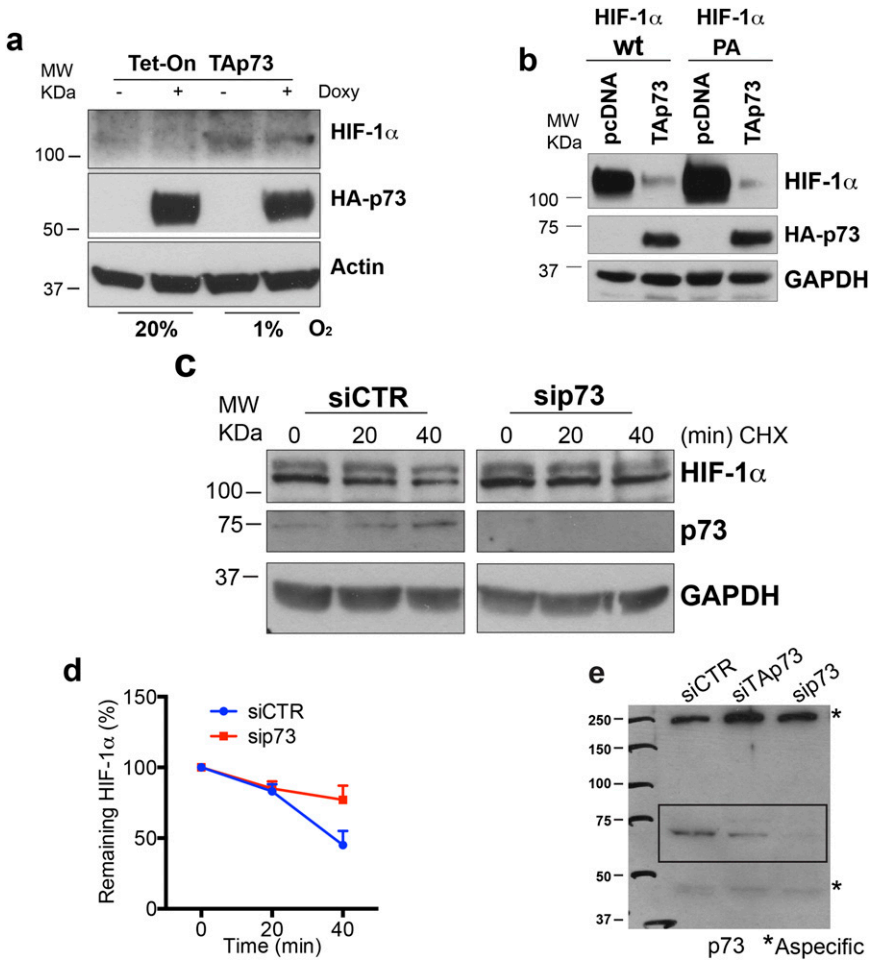


**Fig. S3.** (*A*) Doxycycline-induced TAp73 overexpression in SaOs Tet On cells reduces expression levels of endogenous HIF1α in both normoxic (20% $O_2$) and hypoxic (1% $O_2$) conditions. (*B*) TAp73 overexpression in H1299 can reduce protein level of overexpressed wt HIF-1α and proline/alanine mutant HIF-1α. (*C* and *D*) p73 knockdown increases the HIF-1 protein half-life in H1299 cells. Endogenous HIF-1α was stabilized from oxygen-dependent degradation with a 4-h, 100-μM cobalt chloride treatment. A time-course of 100 μM cycloheximide (CHX) treatment was used to analyze the HIF-1α half-life. Western blots for actin or GAPDH were used as loading controls. (*E*) Full scan of Western blot anti-p73 from Fig. 2*A* shows that TAp73alfa isoform is the only TP73 gene-detectable isoform at protein level in H1299.

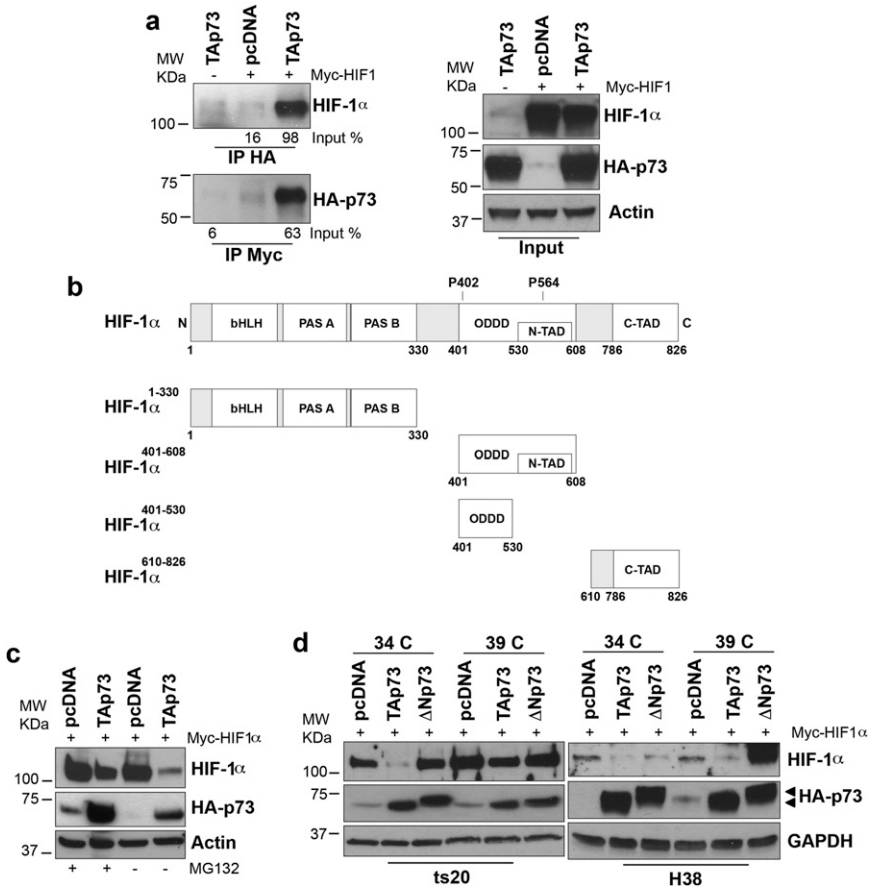


**Fig. S4.** (*A*) Coimmunoprecipitation in H1299 cells of HA-TAp73 and Myc-HIF1α in either direction confirmed the protein interaction. (*B*) Schematic representation of HIF-1α fragments generated to map the interaction site between TAp73 and HIF-1α. (*C*) Proteasome inhibition by 20 μM MG132 abrogated TAp73-dependent HIF-1alfa degradation in H1299. (*D*) The ts20 cells, bearing a temperature-sensitive (ts) ubiquitin-conjugating enzyme (E1) mutant, and H38 control cells were transfected with HIF-1α alone or in the presence of TAp73 isoforms. When shifted to 39 °C to inactivate the E1 enzyme, TAp73-dependent HIF-1 degradation was significantly reduced in ts20 cells. Actin or GAPDH were used as loading control.

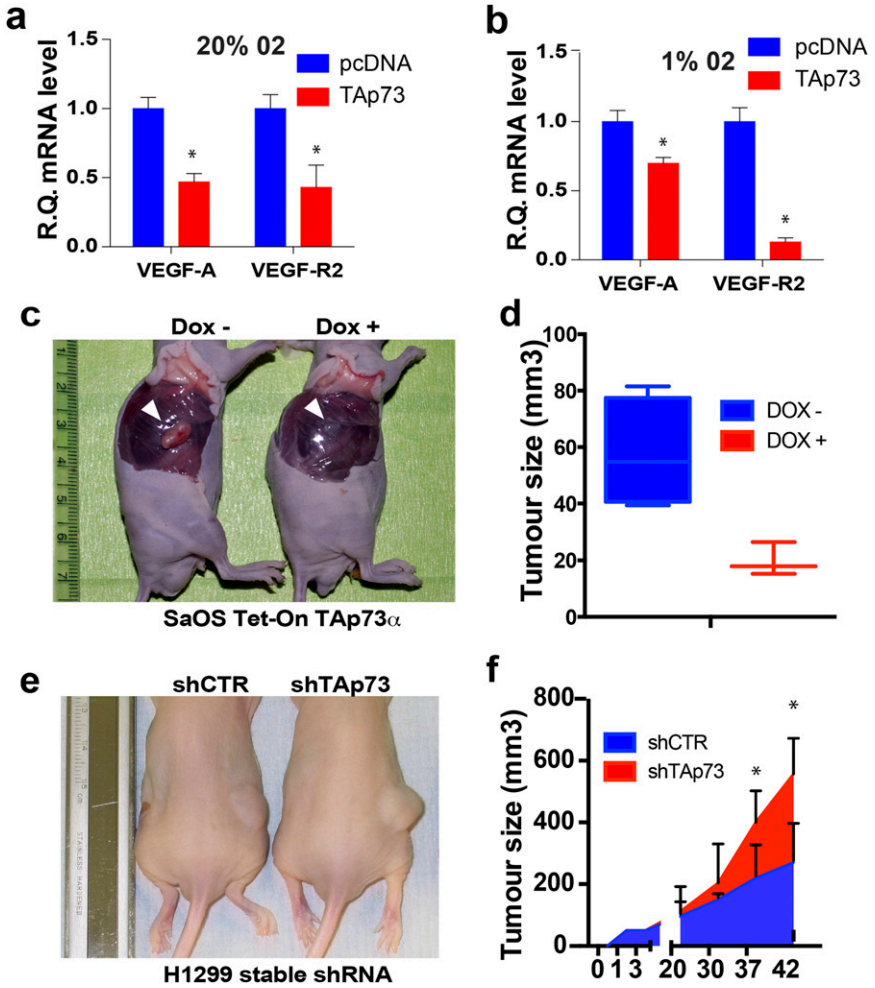


**Fig. S5.** (*A* and *B*) TAp73-overexpressing cells (H1299) displayed a reduced level of the proangiogenic HIF-1a target VEGF-A and the related receptor VEGF-R2 in both normoxic (20% $O_2$) and hypoxic (1% $O_2$) conditions (R.Q. indicates relative quantification (mean ± SD, $n = 3$ independent experiments, two-tailed unpaired *t* test, $*P < 0.01$). (*C*) Tumor derived from xenograft experiment performed by injecting SaOS-2 Tet-onTAp73alfa cells in nu/nu mice: 2 μg/mL of doxycycline was orally administrated to the mice in the water. (*D*) Tumor size was significantly reduced in doxycycline-treated mice ($n = 4$ untreated group, $n = 3$ doxycycline-treated group, two-tailed unpaired *t* test, $P < 0.05$). (*E*) Tumor derived from xenograft experiment performed by injecting shCTR or shTAp73 transfected H1299 in nu/nu mice. (*F*) Tumor size was significantly increased in shTAp73 H1299-derived xenograft tumors ($n = 4$ per group, two-tailed unpaired *t* test, $*P < 0.05$).

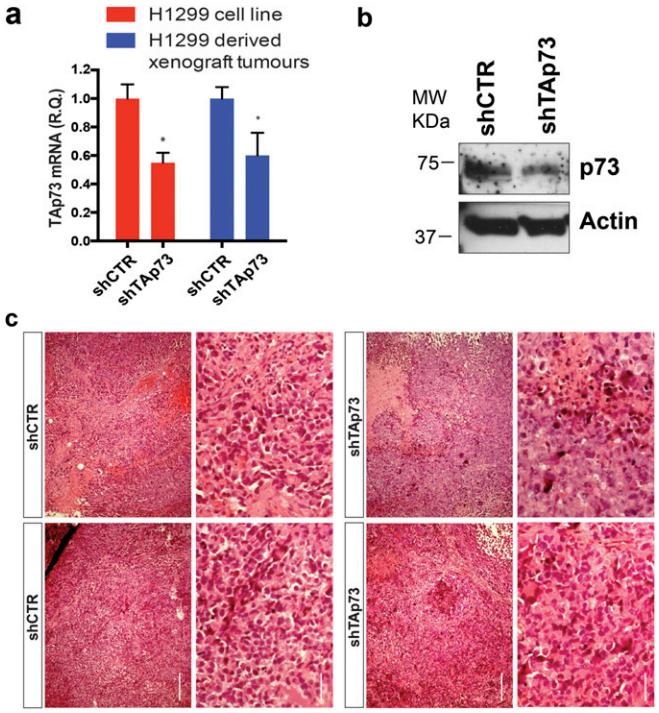


**Fig. S6.** (*A*) qPCR real-time confirmed TAp73 knockdown by mRNA level in stable transfected shTAp73 H1299 cells (R.Q. indicates relative quantification; mean ± SD, $n = 3$ independent experiments, two-tailed unpaired $t$ test, $^*P < 0.05$) and in H1299-derived xenograft tumors ($n = 4$ per group, two-tailed unpaired $t$ test, $^*P < 0.05$). (*B*) Western blot analysis confirmed TAp73 knockdown by protein level in stable transfected shTAp73 H1299 cells. (*C*) Hematoxylin/eosin staining of shCTR or shTAp73 H1299-derived tumor xenograft. (Scale bars, 500 and 100 μm.)

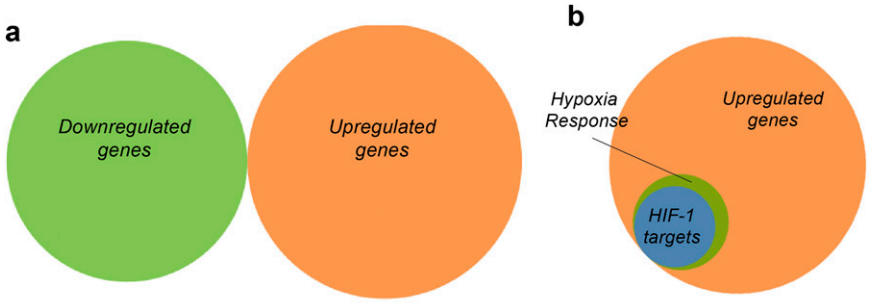


c

| # | GO term | Description | Odds ratio | p-value |
|---|---|---|---|---|
| 1 | GO:0001666 | RESPONSE TO HYPOXIA | 7.12 | 0.01 |
| 2 | GO:0008083 | GROWTH FACTOR ACTIVITY | 5.9 | 0.08 |
| 3 | GO:0042802 | IDENTICAL PROTEIN BINDING | 3.03 | 0.48 |

**Fig. S7.** (*A*) Venn diagram of modulated genes in microarray analysis shown in Fig. 4. Down-regulated genes = 77, up-regulated genes = 123. (*B*) Venn diagram of the most significant enriched pathways within the group of up-regulated genes. (*C*) GO term analysis on gene microarray result shows "Response to Hypoxia" as the highest significant enriched pathway within the up-regulated genes.

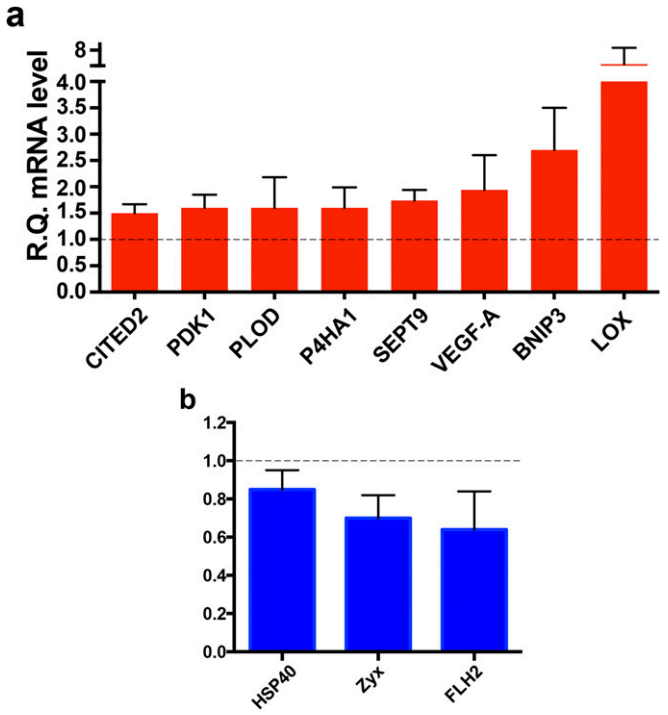


**Fig. S8.** (*A* and *B*) Gene microarray validation by qPCR confirmed the modulation of mRNAs in TAp73-depleted tumors (mean ± SD of $n = 4$ animals per group, two-tailed unpaired *t* test, $P < 0.05$).

## Other Supporting Information Files

Dataset S1 (XLSX)